



# Conditions For "Cold" Gas-Discharge Synthesis of Zinc Oxide And Silver Sulfide Nanostructures Under Automatic Assisting With Ultraviolet Radiation

Alexander Shuaibov, Alexander Minya, Roksolana Hrytsak, Antonina Malinina, Alexander Malinin, Yuriy Zhiguts, Igor Shevera

State Higher Education Institution "Uzhhorod National University", Narodnaya Sq. 3, Uzhhorod, Ukraine

## Correspondence

Alexander Shuaibov

State Higher Education Institution  
"Uzhhorod National University", Narodnaya  
Sq. 3, Uzhhorod, Ukraine

E-mail: alexsander.shuaibov@uzhnu.edu.ua

- Received Date: 19 Mar 2022
- Accepted Date: 25 Mar 2022
- Publication Date: 01 Apr 2022

**Keywords:** critical care, emergency care, children, good strategy

## Copyright

© 2022 Science Excel. This is an open-access article distributed under the terms of the Creative Commons Attribution 4.0 International license.

## Abstract

The characteristics and parameters of the plasma of an overvoltage nanosecond discharge in oxygen, which was ignited between zinc electrodes in oxygen, are presented. Zinc vapors were introduced into the discharge due to microexplosions of natural inhomogeneities on the surfaces of zinc electrodes in a strong electric field. This creates the prerequisites for the synthesis of thin nanostructured zinc oxide films, which can be deposited on a rigid dielectric substrate placed near the electrode system.

The results of a study of the optical characteristics of an overvoltage nanosecond discharge with a discharge gap of  $d=2\text{mm}$  are presented. The identification of the plasma radiation spectra made it possible to establish the main excited plasma products that form the plasma UV radiation spectrum and simultaneously act as a pulsed source of clusters and small particles of zinc oxide.

The characteristics of an overvoltage nanosecond discharge in air between polycrystalline electrodes made of a superionic conductor  $\text{Ag}_2\text{S}$  are presented. In the process of microexplosions of inhomogeneities on the working surfaces of electrodes in a strong electric field, vapors of the  $\text{Ag}_2\text{S}$  compound and its dissociation products in plasma are introduced into the interelectrode space. This creates prerequisites for the synthesis of thin structured films that have the properties of superionic conductors and can be deposited on a dielectric substrate placed near the discharge gap. The spatial, electrical, and spectral characteristics of the discharge, the Raman scattering spectra of the synthesized films, and the homogeneity of their surface are studied.

## Introduction

Zinc oxide is a direct-gap semiconductor with a band gap of about 3.37 eV and an exciton binding energy of  $\sim 60$  meV. It is promising for use as a material for the manufacture of transparent contacts and some other important applications [1–3], photodetectors [4], LEDs [5], in particular, the suitability of nanostructured zinc oxide films for protection was established in [2], from the terrestrial ultraviolet part of the solar spectrum, obtained by a chemical method on inexpensive flexible substrates, and the work presents the results of a study of zinc oxide nanoparticles activated by gamma radiation, which showed that there are no significant changes in the structure of ZnO and they can be used in the treatment of cancer.

In addition to chemical methods for the synthesis of thin nanostructured zinc oxide films, various methods for obtaining such

materials are also widely used. For example, in [6], ZnO:Al thin films were deposited on solid substrates by layer-by-layer deposition in a high-frequency magnetron, and in [7], the results of a study of the structure, morphology, and luminescence of ZnO nanostructures, which were synthesized by electrothermal and electric discharge sputtering, are presented. In a significant number of cases, the method of pulsed laser deposition is also used [8]. Recently, interest has also increased significantly in one-dimensional zinc oxide nanostructures (nanorods, nanowires), since they exhibit size quantum effects, they have a high surface area, which is important for realizing a large absorption capacity of the material, and they are also promising for the development of lasers [9].

A currently less studied method for the synthesis of nanostructured thin films of zinc oxide, when they are deposited from the products of sputtering of zinc electrodes in a

**Citation:** Shuaibov A, Minya A, Hrytsak R, et al. Conditions For "Cold" Gas-Discharge Synthesis of Zinc Oxide And Silver Sulfide Nanostructures Under Automatic Assisting With Ultraviolet Radiation. Biomed Transl Sci. 2022; 2(1):1-8

pulsed discharge of atmospheric pressure and the products of dissociation of a buffer gas (mainly air) [10]. The formation of electrode material vapor occurs at a low average temperature of the discharge device ( $T \leq 100$  C) due to microexplosions of natural electrode inhomogeneities in a strong electric field (ectonic mechanism) [11]. Film synthesis, under these conditions, occurs with automatic assistance of UV radiation from a pulsed discharge plasma [12]. A similar synthesis method using a substrate with a film for UV illumination in the process of its deposition with a separate mercury lamp was used in [13] in the synthesis of zinc oxide nanostructures in the form of a set of nanopillars, which made it possible to reduce the resistance of film nanostructures, in relation to those that were precipitated by UV rays.

Experimental results and characteristics of nanostructured zinc oxide films in air at atmospheric pressure and a mixture of air with water vapor are given in [14–16]. The results of studying the emission characteristics of the plasma of an overvoltage nanosecond discharge in oxygen (at pressure  $p=13.3$  kPa) are given in [17].

To optimize the synthesis of film nanostructures based on zinc oxide, it is important to optimize the operation of such a gas-discharge reactor using not only air at atmospheric pressure, but also oxygen at various pressures. The characteristics of an overvoltage nanosecond discharge between zinc electrodes in oxygen at atmospheric pressure under conditions close to those realized in the experiment have not been previously studied.

The advantage of the pulsed gas-discharge synthesis of zinc oxide nanostructures is that it occurs practically at room temperature of the discharge chamber and makes it possible to deposit films on various biomaterials, fabrics, rubber, and plastics. The use of automatic UV illumination directly from the plasma makes it possible to hope for obtaining transparent

conductive films with lower resistance, which can be used in biomedical engineering and medicine.

The article presents the results of a study of the emission characteristics of an overvoltage nanosecond discharge between zinc electrodes in oxygen; As a result of the sputtering of zinc electrodes and the destruction of oxygen molecules in the plasma, such discharges act as both a source of UV radiation and a flux of zinc oxide clusters and nanoparticles, which can be deposited on a solid substrate installed near the electrode system, which is promising for the synthesis of oxygen oxide films in field of UV radiation. The results of a study of the main characteristics of an overvoltage nanosecond discharge between electrodes based on a polycrystalline superionic conductor  $\text{Ag}_2\text{S}$  in air at atmospheric pressure, as well as the results of a study of the spectra of Raman light scattering by a thin film synthesized from the products of destruction of electrodes in plasma and the surface, are presented.

### Technique and conditions of the experiment

An overvoltage nanosecond discharge was ignited between cylindrical zinc electrodes installed in a dielectric chamber. The block diagram of the experimental device and system for deposition of thin films from the discharge plasma is shown in Figure 1. The distance between the electrodes was 2 mm. The discharge chamber was evacuated with a fore-vacuum pump to a residual pressure of 10 Pa, and then oxygen was admitted into the chamber. The diameter of the cylindrical electrodes was 5 mm; the radius of curvature of their working end surface for both electrodes was 3 mm.

The electrodes were made from zinc or a polycrystalline superionic conductor - silver sulfide ( $\text{Ag}_2\text{S}$ ). The discharge between silver sulfide electrodes was ignited in air at a pressure of 103 kPa.

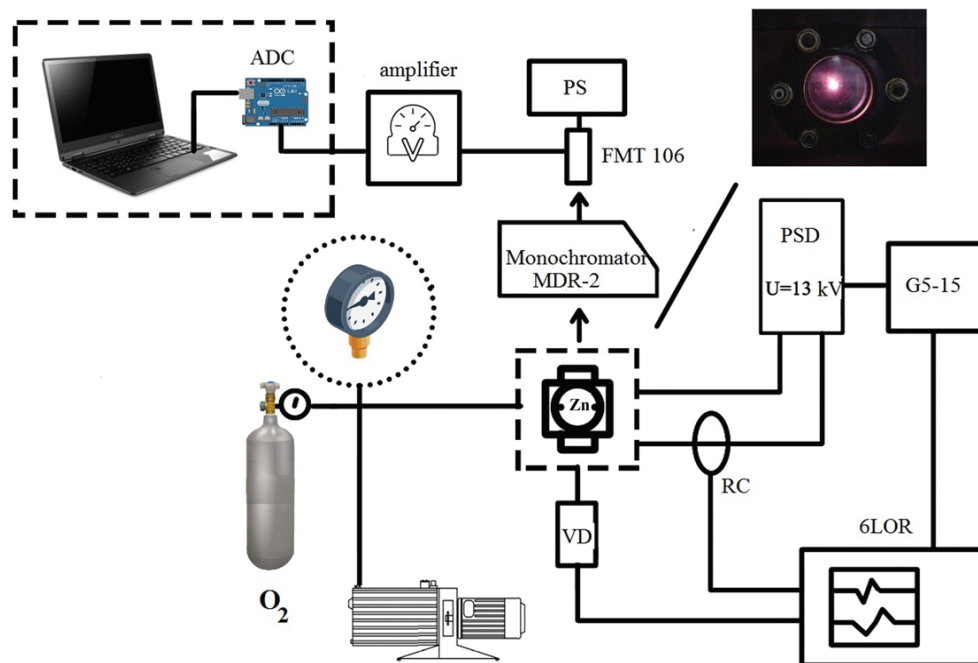


**Figure 1** Diagram of an experimental setup for studying overstressed nanosecond discharge in gases: PSD - discharge power supply; FMT 106 - photoelectric multiplier tube; PS- power supply unit; ADC - analog-to-digital signal converter; RC - Rogovsky coil; VD - voltage divider to determine the voltage drop in the circuit; G5-15 - pulse generator; 6LOR is a broadband oscilloscope.

An overvoltage nanosecond discharge in oxygen was ignited using a high-voltage modulator of bipolar voltage pulses with a total duration of voltage pulses of 50–150 ns at an amplitude of positive and negative components of  $\pm 20$ –40 kV. The frequency of repetition of voltage pulses is 100 Hz. To record the ranges of plasma radiation, an MDR-2 monochromator and a photomultiplier (FEU-106) were used. The signal from the photomultiplier was fed to an amplifier and recorded using an amplitude-to-digital converter in an automated system for measuring spectra on a personal computer display. The discharge radiation was studied in the spectral region 200–650 nm.

### Characteristics of an overvoltage nanosecond discharge

At oxygen pressures in the range of 13.3 and 101.3 kPa, the nanosecond discharge was homogeneous, which is due to the overionization of the gaseous medium from the accompanying X-ray radiation and from the runaway electron beam [19]. The "point discharge" mode was achieved only at voltage pulse repetition frequencies in the range  $f = 40$ –150 Hz, and as the frequency increased to 1000 Hz, the plasma volume of the gas-discharge emitter increased to 100 mm<sup>3</sup>.

The characteristic oscillograms of voltage and current pulses for overvoltage nanosecond discharges between

electrodes in oxygen at atmospheric pressure were close to a similar discharge in air between zinc or copper electrodes [14–16]. The voltage and current oscillograms were in the form of oscillations damped in time with a duration of about 7–10 ns, which is due to a mismatch between the output resistance of the high-voltage modulator and the load resistance. The oscillations of the electrical characteristics were most pronounced on the voltage oscillograms, since the discharge current oscillograms were substantially integrated over time due to the large time constant of the Rogowski coil. The maximum voltage drop across the discharge gap was 30–50 kV, taking into account the positive and negative voltage amplitude. The maximum current amplitude reached 350 A. The highest value of the discharge pulse power was achieved in the first 100–120 ns from the moment of its ignition and reached 4–5 MW. The maximum energy of an individual electric pulse was 100 mJ.

For an overvoltage nanosecond discharge between silver sulfid electrodes in air, the maximum voltage drop across the discharge gap was 40–45 kV. The highest amplitude of the current pulse reached 100 A. The highest value of the discharge pulse power was reached in the first 100 ns from the moment of its ignition and amounted to about 3 MW. The energy of a single electrical impulse was about 77 mJ (Figure 2.).

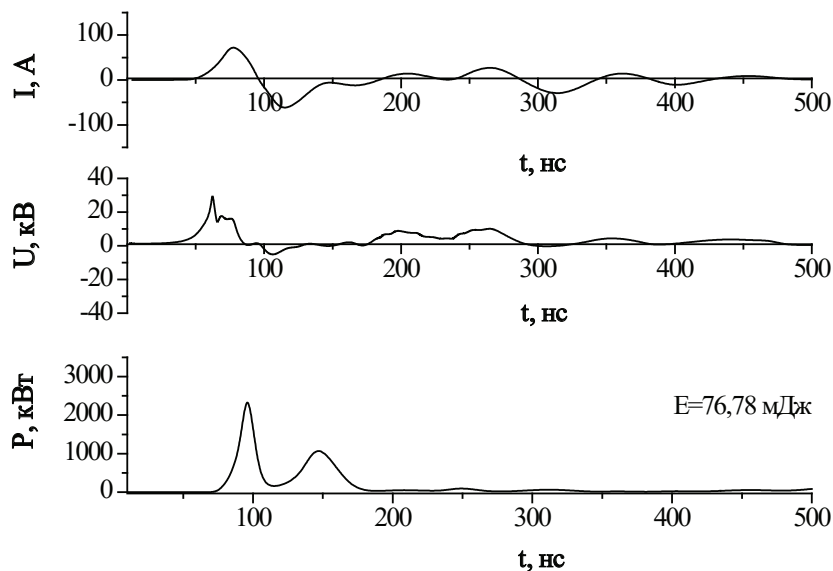


Figure 2. Pulsed power of overvoltage nanosecond discharge in air at pressure  $p=101$  kPa and  $f=1000$  Hz.

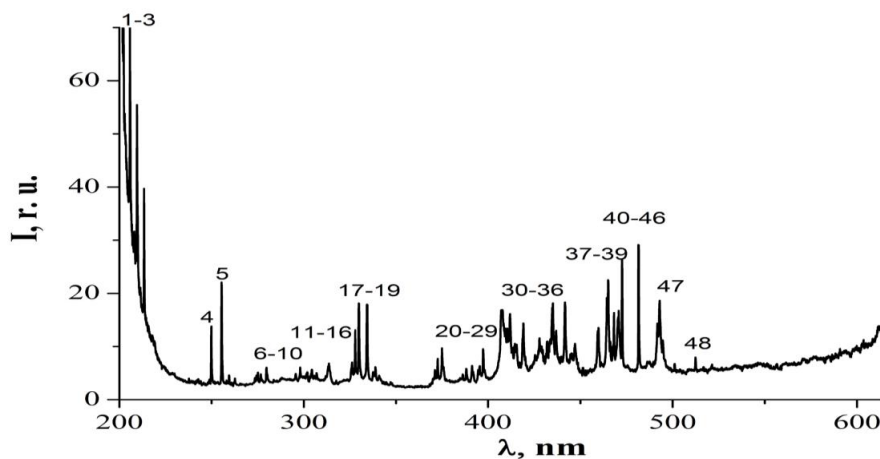


Figure 3. Emission spectrum of an overvoltage nanosecond discharge between zinc electrodes at an oxygen pressure of 101.3 kPa.

**Table 1.** The results of deciphering the emission spectra of an overvoltage nanosecond discharge between zinc electrodes at oxygen pressures of 13.3 and 101.3 kPa.

№	$\lambda_{\text{tab.}}, \text{nm}$	$I_{\text{exp.}}, \text{r.u.}$ $p(\text{O}_2) - 13,3$ $\text{kPa}$	$I_{\text{exp.}}, \text{r.u.}$ $p(\text{O}_2) -$ $101,3 \text{ kPa}$	Object	$E_{\text{low.}}, \text{eV}$	$E_{\text{up.}}, \text{eV}$	Lower <sub>term</sub>	Upper <sub>term</sub>
1	206.20	34.23	72.52	Zn II	0	6.01	$3d^{10}4s$ $^2S_{1/2}$	$3d^{10}4p$ $^2P^0_{1/2}$
2	209.99	35.78	55.72	Zn II	6.11	12.02	$3d^{10}4p$ $^2P^0_{3/2}$	$3d^{10}4d$ $^2D_{5/2}$
3	213.85	23.93	39.54	Zn I	0	5.79	$3d^{10}4s^2$ $^1S_0$	$3d^{10}4s4p$ $^2P^0_1$
4	250.19	10.57	14.38	Zn I	6.01	10.96	$3d^{10}4p$ $^2P^0_{1/2}$	$3d^{10}5s$ $^2S_{1/2}$
5	255.79	18.40	22.59	Zn II	6.11	10.96	$3d^{10}4p$ $^2P^0_{3/2}$	$3d^{10}5s$ $^2S_{1/2}$
6	258.24	2.47	5.22	Zn I	4.02	8.82	$3d^{10}4s4p$ $^3P^0_1$	$3d^{10}4s6d$ $^3D_2$
7	267.05	0.81	3.33	Zn I	4.00	8.64	$3d^{10}4s4p$ $^3P^0_0$	$3d^{10}4s7s$ $^3S_1$
8	273.32	1.36	4.19	O II	25.28	29.82	$2s^22p^2(^3P)3p$ $^2S^{\circ}_{1/2}$	$2s^22p^2(^3P)4s$ $^2P_{3/2}$
9	277.09	2.4	4.54	Zn I	4.02	8.50	$3d^{10}4s4p$ $^3P^0_1$	$3d^{10}4s5d$ $^3D_1$
10	280.08	3.4	6.46	Zn I	4.07	8.50	$3d^{10}4s4p$ $^3P^0_2$	$3d^{10}4s5d$ $^3D_3$
11	298.04	3.31	6.13	O II	28.82	32.98	$2s^22p^2(^3P)3d$ $^4P_{5/2}$	$2s^22p^2(^3P)5f$ $F^2[4]^0_{7/2}$
12	302.01	2.26	5.33	O II	28.83	32.93	$2s^22p^2(^3P)3d$ $^4P_{3/2}$	$2s^22p^2(^3P)5f$ $D^2[3]^0_{5/2}$
13	304.71	2.82	5.67	O II	28.88	32.95	$2s^22p^2(^3P)3d$ $^2F_{7/2}$	$2s^22p^2(^3P)5f$ D $^2[2]^{\circ}_{5/2}$
14	307.206	1.42	5.22	Zn I	4.07	8.11	$3d^{10}4s4p$ $^3P^0_2$	$3d^{10}4s6s$ $^3S_1$
15	313.60	4.71	7.36	N2	The second positive system C3Πu+-B3Πg+ (2;1)			
16	327.75	5.62	13.49	O II	25.83	29.61	$2s^22p^2(^3P)$ $3p$ $4P^0_{3/2}$	$2s^22p^2(^3P)4s$ $4P_{5/2}$
17	329.49	12.89	18.12	O II	25.83	29.59	$2s^22p^2(^3P)3p$ $4P^{\circ}_{3/2}$	$2s^22p^2(^3P)4s$ $4P_{3/2}$
18	334.50	15.89	18.01	Zn I	4.07	7.78	$3d^{10}4s4p$ $^3P^{\circ}_2$	$3d^{10}4s4d$ $^3D_3$
19	339.02	3.57	6.13	O II	25.28	28.94	$2s^22p^2(^3P)3p$ $2S^{\circ}_{1/2}$	$2s^22p^2(^3P)$ $3d$ $2P_{3/2}$
20	340.72	1.95	4.65	O II	28.50	32.14	$2s^22p^2(^1D)3p$ $2D^0_{5/2}$	$2s^22p^2(^1D)$ $4s$ $2D_{3/2}$
21	347.49	2.40	2.40	O II	25.28	28.85	$2s^22p^2(^3P)3p$ $2S^{\circ}_{1/2}$	$2s^22p^2(^3P)3d$ $4D_{1/2}$
22	371.27	2.98	3.18	O II	22.96	26.30	$2s^22p^2(^3P)3s$ $4P_{1/2}$	$2s^22p^2(^3P)3p$ $4S^{\circ}_{3/2}$
23	374.94	7.90	9.86	O II	23.00	26.30	$3s$ $4P_{5/2}$	$3p$ $4S_0$
24	386.34	2.21	4.88	O II	25.64	28.85	$2s^22p^2(^3P)3p$ $4D^0_{5/2}$	$2s^22p^2(^3P)3d$ $4D_{7/2}$
25	388.21	4.07	6.13	O II	25.66	28.85	$2s^22p^2(^3P)3p$ $4D^0_{7/2}$	$2s^22p^2(^3P)$ $3d$ $4D_{7/2}$

26	391.21	3.93	6.58	O II	25.66	28.82	$2s^2 2p^2(^1D)$ $3s^2 D_{3/2}^0$	$2s^2 2p^2(^1D)$ $3p^2 P_{3/2}^0$
27	395.46	3.97	6.69	O I	10.98	14.12	$2s^2 2p^3(^4S^o)$ $3p^3 P_2^o$	$2s^2 2p^3(^2P^o)$ $3s^3 P_2^o$
28	397.32	8.22	9.29	O II	23.44	26.56	$3s^2 P_{3/2}$	$3p^2 P_{1/2}^0$
29	407.58	16.84	16.93	O II	25.65	28.69	$3p^4 D_{5/2}^0$	$3d^4 F_{7/2}$
30	411.92	14.9	12.15	O II	25.85	28.86	$3p^4 P_{5/2}^0$	$3d^4 D_{7/2}$
31	413.28	5.83	9.59	O II	25.83	28.83	$3p^4 P_{1/2}^0$	$3d^4 P_{3/2}$
32	418.97	10.96	14.18	O II	28.36	31.32	$3p'^2 F^0$	$3d'^2 G$
33	431.98	11.70	10.97	O II	28.82	31.69	$2s^2 2p^2(^1D)$ $3p^2 P_{1/2}^o$	$2s^2 2p^2(^1D)$ $3d^2 S_{1/2}$
34	433.68	17.92	17.14	O II	22.98	25.84	$3s^4 P_{3/2}$	$3p^4 P_{3/2}^0$
35	436.92	10.57	13.13	O II	26.22	29.06	$3p^2 D_{5/2}^0$	$3d^2 D$
36	441.48	17.58	18.36	O II	23.44	26.24	$2s^2 2p^2(^3P)$ $3s^2 P_{3/2}$	$2s^2 2p^2(^3P)$ $3p^2 D_{5/2}^0$
37	444.81	3.27	8.80	O II	28.36	31.14	$2s^2 2p^2(^1D)$ $3p^2 F_{7/2}^o$	$2s^2 2p^2(^1D)$ $3d^2 F_{7/2}$
38	446.62	7.03	10.37	O II	28.94	31.73	$3d^2 P_{3/2}$	$4f^4 D_{3/2}^0$
39	459.09	10.39	13.13	O II	25.66	28.36	$3s'^2 D_{5/2}$	$3p'^2 F^0$
40	464.18	15.43	18.89	O II	22.98	25.65	$3s^4 P_{3/2}$	$3p^4 D_{5/2}^0$
41	464.91	21.13	22.17	O II	23.00	25.66	$3s^4 P_{5/2}$	$3p^4 D_{7/2}^0$
42	468.01	9.06	16.40	Zn I	4.00	6.65	$3d^{10} 4s 4p$ $^3 P_0^o$	$3d^{10} 4s 5s^3 S_1$
43	470.53	14.54	17.19	O II	26.25	28.88	$3p^2 D_{5/2}^0$	$3d^2 F_{7/2}$
44	472.21	18.28	26.10	Zn I	4.02	6.65	$3d^{10} 4s 4p$ $^3 P_1^o$	$3d^{10} 4s 5s^3 S_1$
45	481.05	21.35	29.12	Zn I	4.07	6.65	$3d^{10} 4s 4p$ $^3 P_2^o$	$3d^{10} 4s 5s^3 S_1$
46	491.16	5.60	14.05	Zn II	12.01	14.53	$3d^{10} 4d^2 D_{3/2}$	$3d^{10} 4f^2 F_{5/2}^o$
47	492.40	10	18.61	Zn II	12.02	14.53	$3d^{10} 4d^2 D_{5/2}$	$3d^{10} 4f^2 F_{7/2}^o$
48	513.11	3.64	8.48	O I	10.98	13.40	$2s^2 2p^3(^4S^o)$ $3p^3 P_1$	$2s^2 2p^3(^4S^o)$ $8d^3 D_2^o$

In figure 3. the emission spectrum of an overvoltage discharge between zinc electrodes at an oxygen pressure of 101.3 kPa is given, and the emission spectrum of such a discharge at an oxygen pressure of 13.3 kPa at  $d = 2$  mm is given in [17]. The results of the identification of the plasma radiation spectra are given in Table 1. Reference books [20,21] were used to identify individual spectral lines and bands in the discharge radiation spectra.

In the spectral range 206 - 280 nm of radiation from an overvoltage nanosecond discharge based on the Oxygen-Zinc gas-vapor mixture, mainly the spectral lines of zinc (Zn I, Zn II) were recorded. Zn I was distinguished from ionic lines by intensity: 206.20; 209.99, and from atomic spectral lines - 213.85 nm Zn I. A similar intensity distribution of zinc vapor plasma radiation was observed in a gas-discharge lamp [22].

In the emission spectra of plasma of an overvoltage nanosecond discharge between zinc electrodes (at  $d = 1$  mm) in air with a small admixture of water vapor at a mixture pressure of 103.3 kPa, the main ion lines in the UV range of the spectrum were: 202.6; 206.2 nm Zn II, and in the second group the lines of the zinc atom - 250.2; 255.8 nm Zn I [15], which does not correlate with the corresponding results for the discharge in

oxygen (Figure 2 and Table 1). This can be caused by a change in the type of the buffer gas, as well as by the conditions for the formation of ectons under these conditions.

In the spectral region 300 – 500 nm, oxygen ions were the main source of plasma radiation. The most intense spectral lines of a singly charged oxygen ion were the lines: 407.58; 411.92; 433.68; 441.48; 464.18; 464.91 and 470.53 nm O II. The energies of the upper energy states in these oxygen ions reached 25–29 eV, which indicates a high temperature of electrons in an overvoltage nanosecond discharge.

Comparison of the ratio of the effective cross sections of the spectral lines of the zinc atom:  $\lambda = 258.24$  and 267.05 nm, taken from [23], with the experimental data for both gas-vapor mixtures "Oxygen - Zinc" showed that the ratio of the cross sections of the direct electronic excitation of these lines at an electron energy of  $E = 3$  eV was not corresponding to the intensity ratios of these spectral lines obtained in the experiment. It follows from this that the direct electron impact in this experiment is not the main mechanism for populating the upper energy levels for the spectral lines of the zinc atom. Therefore, the most probable mechanisms for the formation of excited zinc atoms, zinc and oxygen ions in an overvoltage

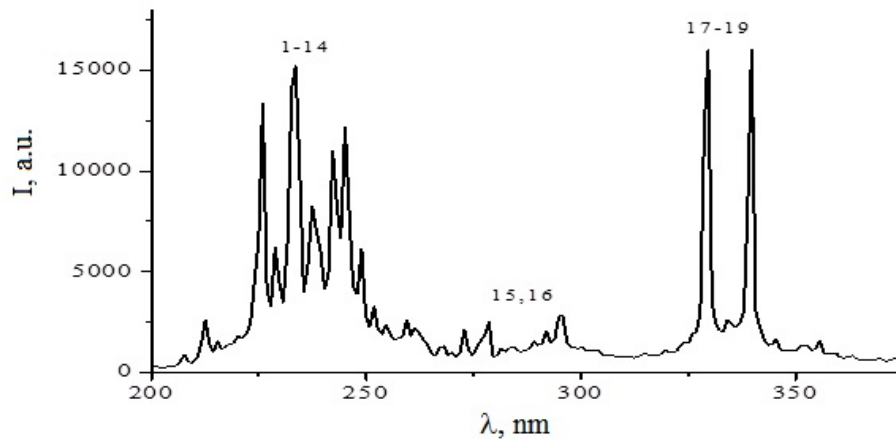


**Figure 4.** Emission spectrum of an overvoltage nanosecond discharge in air at atmospheric pressure.

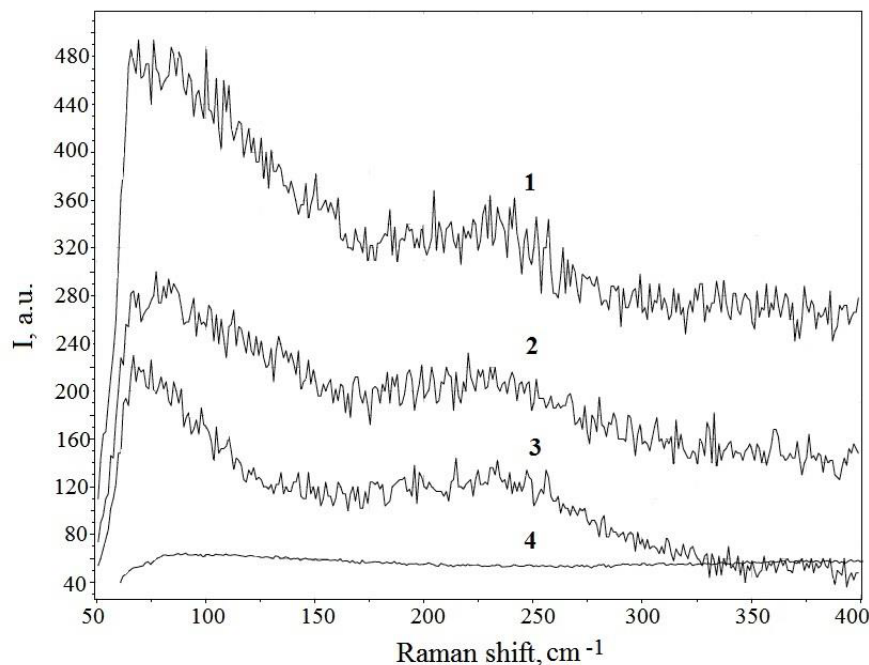


**Figure 5.** Raman emission spectra: 1, 3 - Raman spectra obtained from different parts of the synthesized thin film based on the  $Ag_2S$  superionic conductor; 2 - Raman spectrum of a massive polycrystalline sample from the  $Ag_2S$  compound, from which the electrodes are made, 4 - Raman spectrum of the glass substrate.

nanosecond discharge are due to the processes of their excitation and ionization by electrons from metastable levels, the ground state of the corresponding ion, and dielectronic recombination processes [16].

In Figure 4. The radiation spectrum of a discharge in air between electrodes made of a superionic conductor is shown in the UV region of wavelengths, where the main radiation power of the plasma of this discharge was concentrated.

The investigated plasma radiated intensely in the spectral range 200–350 nm. The main sources of radiation in the short-wavelength spectral range of 200–350 nm were singly charged silver ions (spectral lines 1–16; Figure 3) and silver atoms (lines 17–19) under automatic assistance with UV radiation, which may have a number of advantages in characteristics (lower resistance, etc.) [13].

The Raman spectrum of light scattering by a film synthesized from the products of destruction of electrodes of an overvoltage nanosecond discharge between electrodes from a superionic conductor at atmospheric air pressure is shown in Fig.5. It follows from this figure that the Raman spectra of a thin film are identical with the spectrum of the initial material from which the electrodes are made. Thus, the synthesized thin film should be characterized by the properties of a superionic conductor.

Since the film was synthesized with automatic assistance from plasma UV radiation, it should have a lower resistance compared to the typical synthesis of such films by magnetron sputtering.

Photographs of the surface of thin films based on the  $Ag_2S$  compound using an optical microscope showed that their surface

is fairly uniform. Only individual inhomogeneities with sizes of the order of several micrometers were observed on it, which may be due to the destruction of polycrystalline electrodes in an overvoltage nanosecond discharge. To improve the uniformity of the synthesized films and reduce their synthesis time, it is necessary to reduce the energy in the electric pulse, which can be achieved by reducing the duration of the energy contribution to the plasma, increasing the pulse repetition rate, and also switching to other buffer gases at lower pressures than air at atmospheric pressure.

## Conclusions

Thus, it has been established that an overvoltage nanosecond discharge in oxygen ( $p = 13.3 - 101.3$  kPa) between zinc electrodes ( $d = 2$  mm) is a fairly homogeneous plasma formation with a pulsed electric power up to 5 MW and an energy contribution to the plasma up to 100 mJ.

The study of discharge radiation in gas-vapor mixtures "oxygen-zinc" showed that in the emission spectra of plasma in the wavelength range of 200-650 nm radiation of singly charged zinc and oxygen ions prevailed, and the most intense were the resonant spectral lines of the atom (213.85 nm) and singly charged zinc ion ( $\lambda = 206.20$  nm), as well as a line from  $\lambda = 209.99$  nm Zn I; The emission intensity of the spectral lines of zinc and oxygen increased with an increase in the oxygen pressure; therefore, a discharge at atmospheric oxygen pressures will be most promising for use in automatic assistance in the synthesis of thin films based on zinc oxide nanostructures, which is promising for influencing the electrical characteristics of the synthesized films. Based on the obtained spectral distribution of plasma radiation, the most probable processes for the formation of excited atoms and singly charged ions in this discharge can be reactions of excitation of zinc and oxygen ions by electrons and processes of dielectronic recombination.

The study of the synthesis of thin films of a superionic conductor ( $\text{Ag}_2\text{S}$ ) from the destruction products of electrodes of an overvoltage nanosecond discharge in air at atmospheric pressure revealed the following:

- at a distance between the electrodes of 2 mm, a spatially uniform discharge was ignited, the shape of which was determined by the energy contribution to the plasma and the pulse repetition frequency, which is presumably due to the formation of "runaway electrons" and accompanying X-ray radiation in the discharge, which served as an automatic system of discharge preionization. ;
- the magnitude of the pulsed electric power of the discharge reached 3 MW with an energy in a single pulse of 77 mJ;
- radiation of singly charged silver ions in the spectral range of 200–300 nm and silver atoms in the spectral range of 300–340 nm dominated in the emission spectrum of the discharge plasma, which is promising for the development of a point UV lamp on vapors of the  $\text{Ag}_2\text{S}$  compound for application;
- the study of the spectra of Raman light scattering by thin films synthesized in the experiment showed that they are identical to the corresponding spectra for macroscopic polycrystalline samples from which the electrodes are made; The study of the surface of the synthesized films using an optical microscope revealed their rather high homogeneity.

## References

1. Mridha S, Basak D. Ultraviolet and visible photoresponse

properties of  $\text{ZnO}/\text{Si}-\text{ZnO}/\text{p-Si}$  heterojunction. *Applied Physics*.2007; 101:08102.

2. N.P. Klochko, K.S. Klepikova, D.O. Zhadan, et al. Nanostructured ZnO and CuI Thin Films on Poly(Ethylene Terephthalate) Tapes for UV-Shielding Applications. *J Nano- Electron Phys*. 2020;12(3): 03007.
3. Fedorets I D, Khlopova N P, Dikiy N P, Dovbnaya A N et al 2010 Bulletin of Kharkiv University 916 100.
4. Dae-Kue Hwang, Min-Suk Oh, Jae-Hong Lim and Seong-Ju Park. ZnO thin films and light-emitting diodes 2007 *Journal Of Physics D: Applied Physics* 40 387.
5. Chen C-P, Lin P-H, Chen L-Y, Ke M-Y, Cheng Y-W, Huang JJ. Investigation of light absorption properties and acceptance angles of nanopatterned  $\text{GZO}/\text{a-Si}/\text{p} + \text{-Si}$  photodiodes. *Nanotechnology*. 2009;20:245204.
6. Popovich VI, Yevtushenko AI, Litvin OS, et al. Effect of Argon Deposition Pressure on the Properties of Aluminum-Doped ZnO Films Deposited Layer-by-Layer Using Magnetron Sputtering. *Ukr Phy Journ*. 2016;61(4):325.
7. Burakov VS, Tarasenko NV, Newar EA, Nedelko MI. Morphology and optical properties of zinc oxide nanostructures synthesized by the methods of thermal and discharge sputtering. 2011; 56:245-253.
8. Kurilo IV, Rudy IO, Lopatinsky IY, et al. Bulletin of the National University "Lviv Polytechnic", *Elektronika*. 2011;708:24.
9. Opolchentsev AM, Zadorozhnaya LA, Briskina CM. et al. UV Luminescence and Lasing in Ensembles of Zinc-Oxide Microcrystals with Copper. *Opt Spectrosc*. 2018;125:522–527.
10. Shuaibov OK, Minya AI, Chuchman MP, Malinin AA, Danilo VV, Gomoki ZT. Parameters of Nanosecond Overvoltage Discharge Plasma in a Narrow Air Gap between the Electrodes Containing Electrode Material Vapor. *Journal of Ukrainian Physics*. 2018;63(9):790–801.
11. Mesyats GA. Ecton - an avalanche of electrons from metal. *Usp. Fizich. Nauk*. 1995;165(6):601.
12. Shuaibov AK, Minya AY, Malinina AA. et al. Study into Synchronous Flows of Bactericidal Ultraviolet Radiation and Transition Oxides Metals (Zn, Cu, Fe) in a Pulsed Gas Discharge Overvoltage Reactor Nanosecond Discharge in the Air. *Surf. Engin. Appl.Electrochem*. 2020;56:510–516.
13. Abduev AK, Asvarov AS, Akhmedov AK. et al. UV-assisted growth of transparent conducting layers based on zinc oxide. *Tech Phys Lett*. 2017;43: 1016–1019.
14. Minya OY, Shuaibov OK, Gomoki ZT, Danilo VV, Chavarga MM, Kukri LE. Optical characteristics nanosecond order per sum testing with zinc vapor Bulletin of Uzhgorod University. *Physics*. 2016;39:93.
15. Danilo VV, Minya OI, Shuaibov OK, Shevera IV, Gomoki ZT, Dudich MV. *Scientific Bulletin of Uzhgorod University. Physics*. 2017;42:128.
16. Shuaibov OK, Malinina AO. Overstressed Nanosecond Discharge in the Gases at Atmospheric Pressure and Its Application for the Synthesis of Nanostructures Based on Transition Metals. *Progress in Physics of Metals*. 2021;22(3):382–439.
17. Vatralla M I, Grytsak R V, Malinina A O, Kudin O O, Shuaibov O K Book of abstracts. International Conference of Young Scientists and Post Graduate Students. Uzhhorod, 26–28 May 2021148.
18. Korytchenko KV, Shypul OV, Samoilenko D, et al. Numerical simulation of gap length influence on energy deposition in spark discharge. *Electrical Engineering & Electromechanics*. 2021;2021(1): 35-43.
19. Tarasenko VF. Runaway electrons preionized diffuse discharge. Science Publishers Inc., New York. 2014.

20. Striganov AR. Tables of spectral lines of neutral and ionized atoms. IFI/Plenum M.: Atomizdat, New York. 1966.
21. NIST Atomic Spectra Database Lines Form [https:// physics.nist.gov/ PhysRefData/ASD/lines\\_form.html](https://physics.nist.gov/PhysRefData/ASD/lines_form.html)
22. Maksimov S, Kretinina AV, Fomina NS, Gall LN. Combined radiator for spectrophotometer in the spectral range from 200 to 1100 nm. Scientific Instrumentation. 2015; 25(1):36-41.
23. Smirnov YM. Electron-impact excitation of triplet levels of the zinc atom. Opt Spectrosc. 2008;104(2):159-164.